



Improving photocatalytic water reduction activity for In_2TiO_5 by loading metal cocatalysts



Kai Song^a, Jia Yang^a, Yu Sun^b, Ziyao Wang^b, Ling Wang^b, Rihong Cong^a, Tao Yang^{a,*}

^a College of Chemistry and Chemical Engineering, Chongqing University, Chongqing 400044, PR China

^b Bashu Secondary School, Chongqing 400013, PR China

ARTICLE INFO

Article history:

Received 28 April 2015

Received in revised form

6 June 2015

Accepted 11 June 2015

Available online 21 June 2015

Keywords:

Oxide materials

Semiconductors

Solid state reactions

Catalysis

X-ray diffraction

ABSTRACT

In_2TiO_5 is the only ternary oxide in the In–Ti–O phase diagram. It was prepared by high temperature solid state reaction in this work and verified to be pure with high crystallinity by Le Bail fitting on the powder X-ray diffraction (XRD) pattern. Scanning electron microscopy show that the micrometer particles of In_2TiO_5 was composed of submicron crystallites. UV–vis diffused reflectance spectra suggested a wide bandgap of 3.55 eV, which is consistent with the theoretical calculations. The bottom of the conduction band is composed of both In 6s and Ti 3d orbitals, however the low density of the states lead to a low density of the charge carriers excited by UV irradiation. Thus the photocatalytic H_2 production rate of In_2TiO_5 is only 3.6 $\mu\text{mol}/\text{h}/\text{g}$ in 20 vol% methanol aqueous solution. With the assistance of Ru- and Pt-cocatalyst, the activity is significantly increased and the optimal H_2 evolution rate is 35.7 $\mu\text{mol}/\text{h}/\text{g}$ when loading 1 wt% Ru and 1 wt% Pt, simultaneously. All the catalysts recovered after the photocatalytic reactions show no degradation according to powder XRD.

© 2015 Elsevier B.V. All rights reserved.

1. Introduction

Photocatalytic water reduction is a green and promising technique to convert the solar energy into the chemical form of H_2 , and the first pronounced work was the photo-electrochemical water reduction using UV-excited TiO_2 in 1972 [1]. Thereafter, TiO_2 was the most extensively studied photocatalyst which can catalyze the production of hydrogen and/or oxygen from water vapor, pure water, and aqueous solutions containing electron donors [2–4]. Especially, TiO_2 loaded with ultrafine Pt and RuO_2 particles can generate H_2 and O_2 in the stoichiometric proportion from water, and the apparent quantum yield achieved 30% at 310 nm [5]. Various titanates, including $\text{Na}_2\text{Ti}_3\text{O}_7$, $\text{K}_2\text{Ti}_4\text{O}_9$, $\text{Cs}_2\text{Ti}_2\text{O}_5$, $\text{Cs}_2\text{Ti}_5\text{O}_{11}$, $\text{M}_2\text{Ti}_6\text{O}_{13}$ ($M = \text{Na}, \text{K}, \text{Rb}, \text{Cs}$), MTiO_3 ($M = \text{Ca}, \text{Sr}, \text{Ba}$), and $\text{Ln}_2\text{Ti}_2\text{O}_7$ ($\text{Ln} = \text{Y}, \text{La}, \text{Pr}, \text{Nd}, \text{Sm}–\text{Lu}$), are also good photocatalysts for H_2 production from aqueous solution under UV irradiation [6,7]. Hence, the Ti-containing semiconductors are considered to have high potentials in heterogeneous photocatalysis.

On the other hand, $\text{In}_{1-x}\text{Ni}_x\text{TaO}_4$ was reported as the first photocatalyst, which is capable of overall water splitting under visible

light [8]. It is therefore a natural idea to investigate In_2TiO_5 , which is the only ternary compound in the In–Ti–O phase diagram at high temperature. The crystal structure is composed of six-coordinated In and Ti. For example, InO_6 and TiO_6 octahedra connect with each other by either edge- or corner-sharing as shown in Fig. 1 [9]. The three dimensionality of the metal-oxygen ionic framework is supposed to be benefit to the charge migration, which is the prerequisite for photocatalysis.

In 2007, the photocatalytic property of In_2TiO_5 was studied by Huang for the first time, where it could photocatalyze the degradation of methyl orange (MO) and the catalytic activity was higher than that of TiO_2 (P25) [10]. Thereafter in 2011, N-doped In_2TiO_5 was used for the decomposition of Rhodamine B (RhB) under visible light irradiation [11]. Wu also reported the intrinsic activity of In_2TiO_5 to the photodegradation of C.I. Reactive Red 2 (RR2) under visible light in 2014 [12]. With regards to the ability of photocatalytic water reduction, $\text{In}_2\text{Ti}_{1-x}\text{V}_x\text{O}_{5+\delta}$ was applied to splitting water but not in stoichiometric ratio of H_2 and O_2 , under visible light or UV irradiation in 2009 [13]. However, it is a bit questionable about the phase purity of $\text{In}_2\text{Ti}_{1-x}\text{V}_x\text{O}_{5+\delta}$. The chemical synthesis for $\text{In}_2\text{Ti}_{1-x}\text{V}_x\text{O}_{5+\delta}$ was supposed to be performed in the vacuum system to avoid the evaporation and oxidation problem of vanadium. While the authors carried out the heating procedure in air and the powder X-ray diffraction (XRD) together with the

* Corresponding author.

E-mail address: taoyang@cqu.edu.cn (T. Yang).

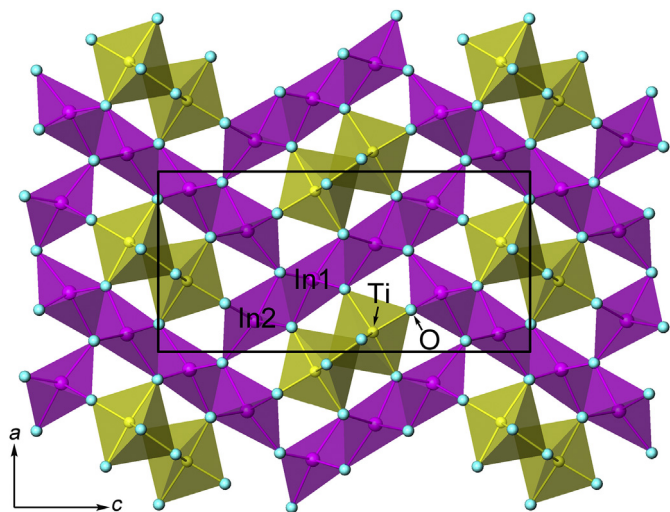


Fig. 1. Representative structure view of In_2TiO_5 along the b -axis. The unit cell is shown as the black rectangle.

refinements are not appropriately interpreted. Anyway, it was a good sign that In_2TiO_5 might be a good catalyst for water splitting. In literature, there was another presumably existed solid solution $\text{In}_{2(1-x)}\text{Nd}_{2x}\text{TiO}_5$ showing photocatalytic water reduction ability [14]. Recently, Bharadway and his coworkers studied the photocatalytic H_2 generation over both bulk and nano-sized In_2TiO_5 in aqueous solution [15]. Here we synthesized In_2TiO_5 by high temperature solid state reaction. The bulk phase was characterized by powder XRD, scanning electron microscopy, UV–vis diffused reflectance spectroscopy, and X-ray photoelectron spectra. Theoretic calculations suggest the bottom of the conduction band (CB) is mainly contributed by both In 6s and Ti 3d orbitals. In addition, photocatalytic activities of H_2 production over as-prepared and especially, the cocatalyst-loaded In_2TiO_5 were investigated, where the optimal H_2 evolution rate is $35.7 \mu\text{mol/h/g}$ under UV-light irradiation.

2. Materials and methods

2.1. Preparations of the catalysts

High temperature solid state reaction was applied to synthesize In_2TiO_5 bulk samples. Generally, a stoichiometric mixture of starting materials (TiO_2 and In_2O_3) was homogenized using an agate mortar and followed by a preheating at 800°C for 10 h. The resultant powder was re-ground thoroughly by hands and pressed into a pellet in the diameter of 13 mm. The pellet was finally heated at 1050°C for another 15 h in air.

In this work, 1 wt% Pt and/or 1 wt% Ru were used as cocatalysts to improve the photocatalytic activity of In_2TiO_5 . For example, 0.20 g In_2TiO_5 , 1.4 mL of $\text{H}_2\text{PtCl}_6 \cdot 6\text{H}_2\text{O}$ in the concentration of 1.48 mg/mL (or 2.1 mL of RuCl_3 in the concentration of 0.97 mg/mL), and 10 mL of distilled water were placed in a 100 mL beaker. This solution was mixed by ultrasonication for 20 min. A dilute aqueous KBH_4 was added to the solution very slowly to obtain Pt (or Ru) particles. The obtained samples were generally gray or close-to-black powder, which were washed with water and dried at 60°C in an oven before further characterization.

2.2. Characterizations

Powder XRD data were collected on a PANalytical X'pert

diffractometer equipped with a PIXcel 1D detector (Cu $K\alpha$ radiation, 1.5406 \AA). The operation voltage and current are 40 kV and 40 mA, respectively. Le Bail refinements were performed to obtain the cell parameters using TOPAS software package [16]. Scanning electron microscopy (SEM) was performed on JEOL-7800F at an accelerating voltage of 5.0 kV, and the working distance is 4.1 mm. UV–vis diffused reflectance spectrum (DRS) was recorded by Shimadzu UV-3600 spectrometer equipped with an integrating sphere attachment. The analysis range was from 200 to 1200 nm, and BaSO_4 was used as reflectance standard. X-ray photoelectron spectra (XPS) were acquired with UK Kratos Axis Ultra spectrometer with Al $K\alpha$ X-ray source operated at 15 kV and 15 mA. Electron binding energies were calibrated against the C 1s emission at $E_b = 284.8 \text{ eV}$ to correct the contact potential differences between the sample and the spectrometer.

2.3. Theoretical calculations

Theoretical studies on In_2TiO_5 is operated by the Vienna *ab-initio* simulation package (VASP) [17]. The projector augmented-wave (PAW) method implemented in the VASP code was utilized to describe the interaction between the ionic cores and the valence electrons [18]. The generalized gradient approximation (GGA) parameterized by Perdew, Burke, and Ernzerhof (PBE) was employed to describe the exchange-correlation potential in the standard DFT calculations [19]. For single point energy and density of states, a cutoff energy of 500 eV for the plane-wave basis and $1 \times 2 \times 1$ Monkhorst-Pack G-centered k -point meshes were employed.

2.4. Photocatalytic activity evaluation

Photocatalytic activities were tested on a gas-closed circulation system equipped with a vacuum line (LabSolar-IIIAG system, Perfect Light Ltd. Co.), a 150 ml Pyrex glass reactor and a gas sampling port that is directly connected to a gas chromatograph (Shanghai Techcomp-GC7900, TCD detector, molecular sieve 5A, N_2 gas carrier). In a typical run, 50 mg of catalyst was dispersed by a magnetic stirrer in 50 mL of 20 vol% methanol aqueous solution. The solution was kept been stirred, and a 5°C cycling water bath was applied to keep the reaction vessel at a constant temperature. The light irradiation source was generated by an external 500 W Hg-lamp (CEL-M500, Beijing AuLight Ltd. Co.).

3. Results and discussion

The Le Bail fitting of the whole XRD pattern for as-prepared In_2TiO_5 was presented in Fig. 2a. Apparently, there is no observable impurity and the reflection peaks possess sharp profiles which indicate the high crystallinity of the sample obtained by high temperature annealing. The final refined cell parameters are $a = 7.242 \text{ \AA}$, $b = 3.503 \text{ \AA}$, $c = 14.894 \text{ \AA}$ in the space group $Pnma$. As shown in Fig. 3, the SEM images indicate the obtained powder sample are micrometer particles which are in fact composed of sub-micron crystallites. In addition, the smooth surface of the particles also suggest the high crystallinity, in consistent with the XRD analysis. Keeping stable under high density beam of incident irradiation is vital for a heterogeneous photocatalyst. Fig. 2b shows the XRD patterns for those samples (with or without loading cocatalysts) before and after the photocatalytic reactions in methanol aqueous solution for several hours. No observable degradation can be found, proving that In_2TiO_5 is intrinsically stable under UV-irradiation.

UV–vis diffused reflectance spectroscopy is an effective technique to investigate the bandgap energies of semiconductors,

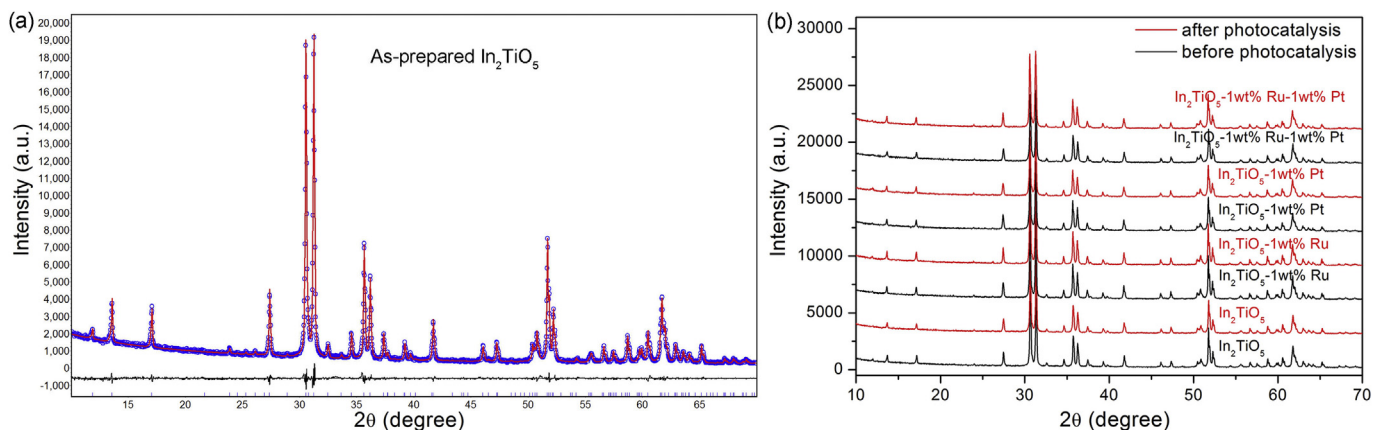


Fig. 2. (a) Le Bail fitting for as-prepared In_2TiO_5 . The blue symbol \circ represents observed data and the red solid line is the calculated pattern; the blue marks below the diffraction patterns are the expected reflection positions, and the difference curve is also shown as black curves at the bottom. (b) Powder XRD patterns for those samples before and after photocatalytic reactions. (For interpretation of the references to colour in this figure legend, the reader is referred to the web version of this article.)

which correspond to electron excitation from valance band (VB) to conduction band (CB). As shown in Fig. 4, the absorption band of In_2TiO_5 lies mainly in the UV region and there is a steep edge, which

indicates the absorption band is not due to the transition from impurity energy levels but the bandgap transition [20]. In addition, the co-catalysts loaded samples show similar DRS patterns (see Fig. 4), the only difference is the relatively stronger absorbance in the visible light region, which is due to the color of Pt/Ru nanoparticles on the surface. For most semiconductors, the dependence of the absorption coefficient α on the bandgap energy E_g can be expressed by the following equation: $Ah\nu = A(h\nu - E_g)^{n/2}$, where h , ν , and A are Planck constant, light frequency, and proportionality, respectively; n is determined on the basis of the transition type (i.e. $n = 1$ for direct transition, $n = 4$ for indirect transition). The plot of $(\alpha h\nu)^2$ [2] against $h\nu$ (assuming it is a direct transition) is shown in the insert of Fig. 4. The extrapolated value of $h\nu$ at $\alpha = 0$ gives an absorption edge energy corresponding to E_g , which is 3.55 eV for In_2TiO_5 . Note that the reported value of the bandgap is in the range of 3.02–3.9 eV in literature [10–15], where the difference came from the different morphology of the so-prepared sample.

In fact, X-ray photoelectron spectra were collected for all samples studied in this work (see Fig. 5). In^{3+} and Ti^{4+} were confirmed to be consistent in all samples within the experimental error. The loaded cocatalysts were at a mass fraction of 1% and the signals were generally weak. The valence state of Pt is confirmed to be zero,

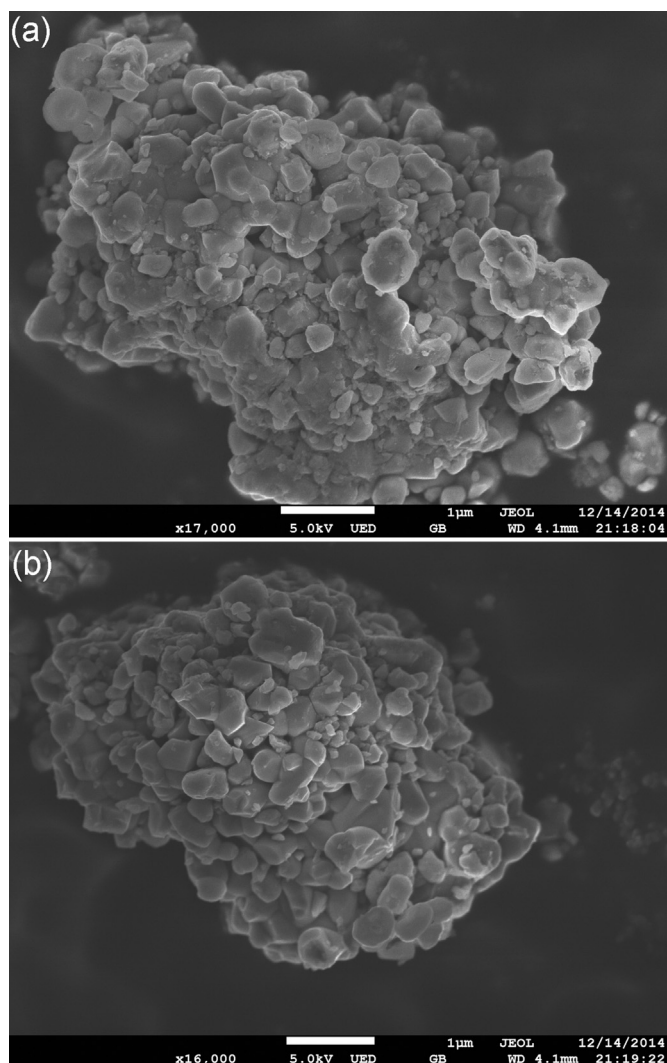


Fig. 3. SEM images for In_2TiO_5 .

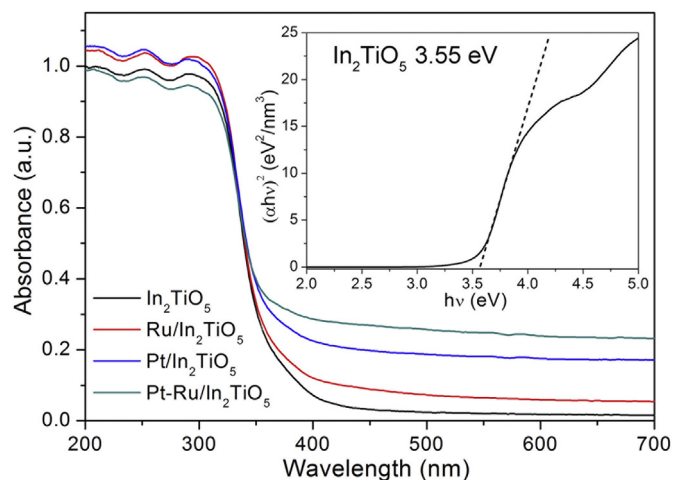


Fig. 4. UV-vis diffused reflectance spectra for In_2TiO_5 with and without co-catalysts loading and the insert shows the plot of $(\alpha h\nu)^2$ against photon energy ($h\nu$). The estimated bandgap energy is 3.55 eV.

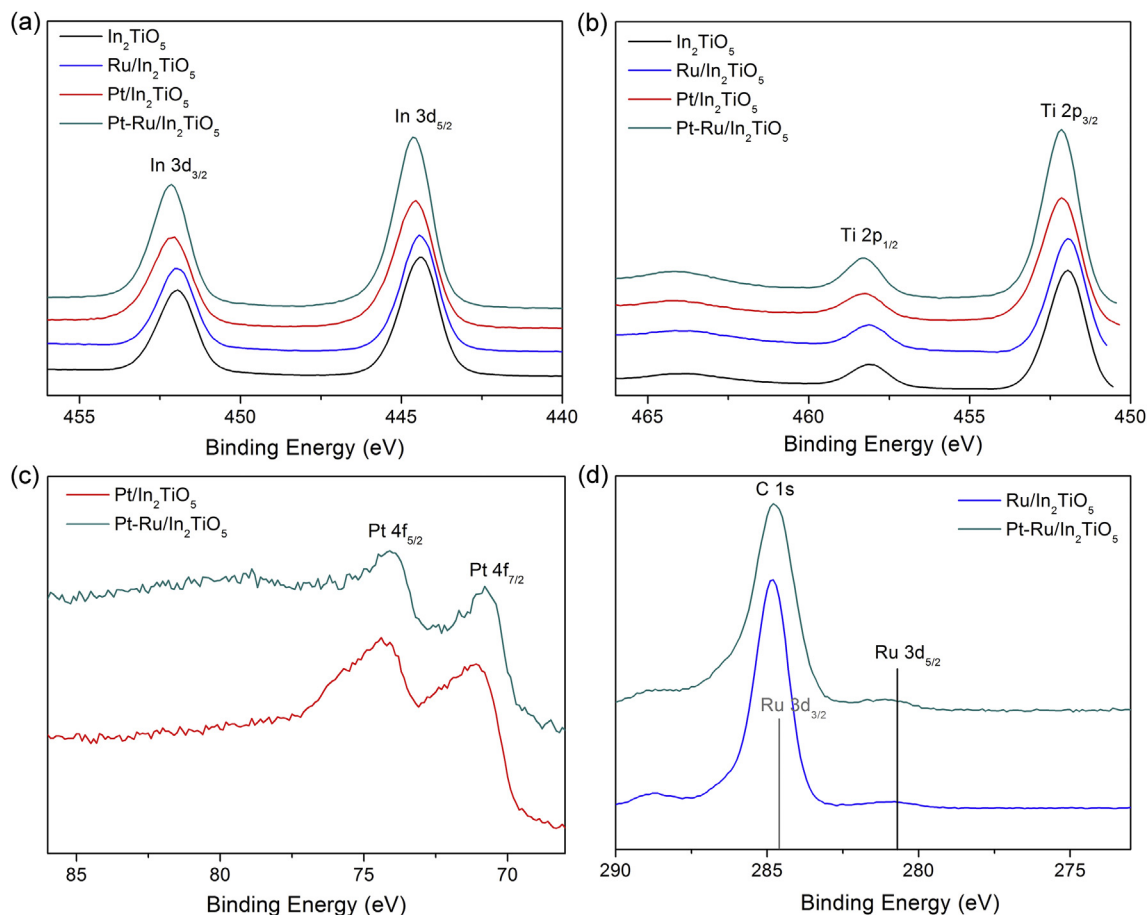


Fig. 5. XPS data for In_2TiO_5 with and without co-catalysts loading, which confirms the presence of In^{3+} , Ti^{4+} , Pt and Ru^{4+} .

which is as expected. However, the major peak of Ru ($3d_{3/2}$) is overlapped with the C 1s emission at 484.8 eV, thus only a tiny single was observed at the supposed position of Ru $3d_{5/2}$ (see Fig. 5d). Nevertheless, the observed binding energy of Ru suggested

the formation ruthenium dioxide.

The calculated density of states for In_2TiO_5 was presented in Fig. 6, which helps the understanding of the photocatalytic property. As indicated, the bandgap energy is about 2.03 eV, which is

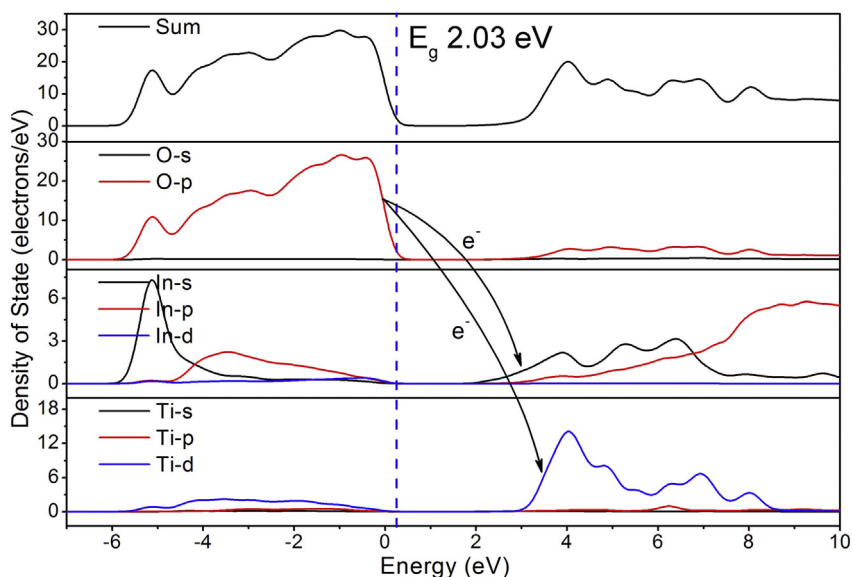


Fig. 6. Theoretical calculations of the density of states for In_2TiO_5 . The calculated bandgap energy is 2.03 eV. It is schemed that the electrons can be photo-excited from O 2p orbitals to In 6s and Ti 3d orbitals.

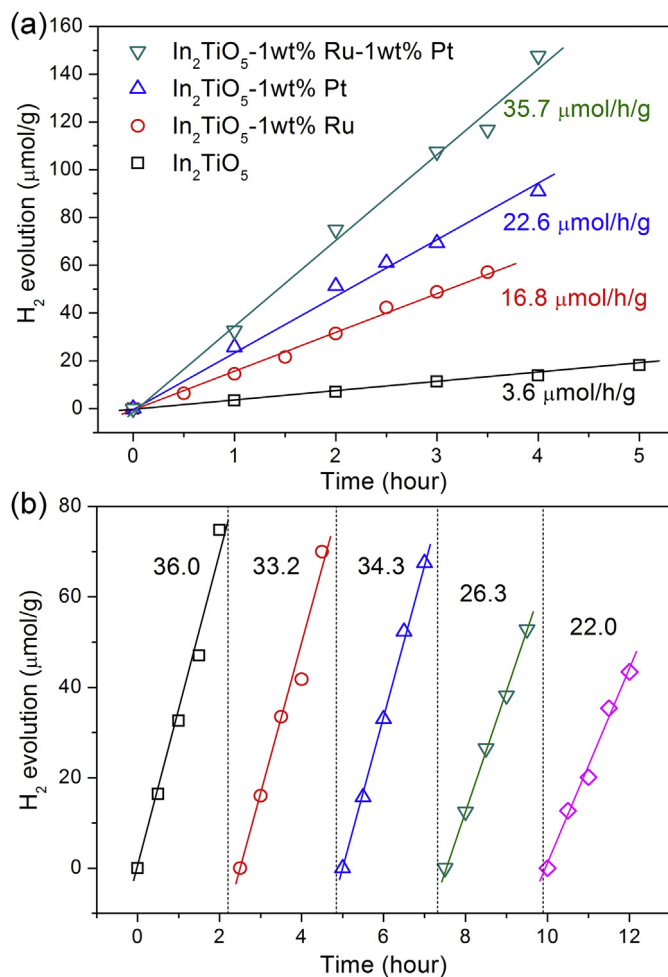


Fig. 7. (a) photocatalytic H₂ evolution from 20 vol% methanol aqueous solution under UV-irradiation. The photocatalysts include the as-prepared In₂TiO₅ and those loaded with 1 wt% Ru and/or 1 wt% Pt. The straight lines are just guide for eyes. (b) A long term photocatalytic reaction over In₂TiO₅ loaded with 1 wt% Ru and 1 wt% Pt. The H₂ evolution rate decreases after 3 cycles, which is interpreted to be due to the loss of the cocatalyst.

smaller than the experimental value estimated by DRS. It is due to the discontinuity of the XC energy during the calculations and is commonly seen. The top of the VB is mostly consisted of O 2p orbitals, which is a common feature for metal oxides. The very bottom of the CB is contributed by the empty In 6s orbitals, however, with a relatively low density. In fact, the majority of the CB bottom is composed of unoccupied Ti 3d orbitals. According to the calculations, we speculate that the photocatalytic mechanism of In₂TiO₅ as follows. Electrons in the O 2p orbitals are prompted to the excited states, which is composed of In 6s and Ti 3d orbitals, thereafter, the active electrons migrate through the metal-oxygen ionic framework to the surface of the particle for catalytic reactions.

The photocatalytic activities of various photocatalysts were evaluated with the model reaction of photocatalytic H₂ production as shown in Fig. 7. With the assistance of CH₃OH as sacrificial reagents, the H₂ production rate of as-prepared In₂TiO₅ is 3.6 μmol/h/g. First, the low efficiency is largely due to the high level of charge recombinations during the migration process, and second, the theoretical study shows that the very bottom of CB has a low density from In 6s orbitals, which would lead to a low carrier density.

Loading cocatalyst is always an effective post-treatment to

enhance the catalytic activity. After loading 1 wt% Ru and 1 wt% Pt, the H₂ production rates were improved to 16.8 and 22.6 μmol/h/g, respectively. Usually, negative charged electrons would accumulate at Pt sites because of its relatively low Fermi level [21], while the loaded Ru can play a role of the collector for positive charged holes [22]. In addition, these cocatalysts provide abundant catalytic sites, which usually have strong binding ability to substrates. Here, the photocatalytic activity of Pt-loaded sample is slightly higher than the Ru-loaded one, which means improving the migration of the electrons has a more important influence to the photocatalytic activity.

Furthermore, the bimetallic cocatalyst loading (with 1 wt% Pt and 1 wt% Ru) offered a higher H₂ evolution rate of 35.7 μmol/h/g (see Fig. 7). Probably a synergetic effect occurs when loading two types of cocatalysts. We performed an extended experiment over this catalyst for 5 cycles. After each cycle the system was evacuated. The activity started to decline after 3 cycles. Nevertheless, the activity was still much higher than the host In₂TiO₅. The XRD pattern after the 5-cycle reaction shows no difference with the as-prepared sample (see Fig. 2b), thus we interpret that the decrease of the activity is due to the loss of cocatalyst from the surface. From this aspect, more effects are needed to improve the loading technique of cocatalyst, which usually requires a compact combination with the host.

4. Conclusions

We prepared In₂TiO₅ by high temperature solid state reaction. Le Bail fitting on powder XRD verified high purity and crystallinity of the as-prepared sample, and the SEM images show the micrometer particles composed of submicron crystallites. DRS and theoretical calculations suggest the wide bandgap characteristic and the observed bandgap is 3.55 eV assuming the direct semiconductor model. The top of the VB is contributed by O 2p orbitals, and the bottom of the CB is composed of by both In 6s and Ti 3d orbitals. The UV-irradiated H₂ evolution rate for In₂TiO₅ is 3.6 μmol/h/g. The very low activity is due to the low density of the charge carrier according to the calculated density of states at CB as well as the high level of charge recombination during the migration process. The Ru- and Pt-cocatalyst loading improved the H₂ evolution rate to 16.8 and 22.6 μmol/h/g, respectively. Moreover, 1 wt% Ru together with 1 wt% Pt loaded In₂TiO₅ show a superior activity of 35.7 μmol/h/g. Our study proves the photocatalytic water reduction property of In₂TiO₅ and our preliminary attempt of cocatalyst loading indeed improved the activity.

Acknowledgment

This work was financially supported by the Nature Science Foundation of China (Grants 91222106, 21171178) and Natural Science Foundation Project of Chongqing (Grants 2012jjA0438, 2014jcyjA50036). We also acknowledge the support from the sharing fund of large-scale equipment of Chongqing University.

References

- [1] A. Fujishima, K. Honda, *Nature* 238 (1972) 37–38.
- [2] X.B. Chen, S.S. Mao, *Chem. Rev.* 107 (2007) 2891–2959.
- [3] X.B. Chen, L. Liu, F.Q. Huang, *Chem. Soc. Rev.* 44 (2015) 1861–1885.
- [4] F.E. Osterloh, *Chem. Soc. Rev.* 42 (2013) 2294–2320.
- [5] D. Duonghong, E. Borgarello, M. Graetzel, *J. Am. Chem. Soc.* 103 (1981) 4685–4690.
- [6] X.B. Chen, S.H. Shen, L.J. Guo, S.S. Mao, *Chem. Rev.* 110 (2010) 6503–6570.
- [7] A. Kudo, Y. Miseki, *Chem. Soc. Rev.* 38 (2009) 253–278.
- [8] Z.G. Zou, J.H. Ye, K. Sayama, H. Arakawa, *Nature* 414 (2001) 625–627.
- [9] J.W. Tang, Z.G. Zou, J.H. Ye, *Chem. Mater.* 16 (2004) 1644–1649.
- [10] W.D. Wang, F.Q. Huang, C.M. Liu, X.P. Lin, J.L. Shi, *Mat. Sci. Eng. B* 139 (2007)

- 74–80.
- [11] Y. Liu, G. Chen, C. Zhou, Y.D. Hu, D.G. Fu, J. Liu, Q. Wang, *J. Hazard. Mater.* 190 (2011) 75–80.
- [12] C.H. Wu, C.Y. Kuo, C.H. Lai, W.Y. Chung, *Reac. Kinet. Mech. Cat.* 111 (2014) 383–392.
- [13] P. Shah, D.S. Bhange, A.S. Deshpande, M.S. Kulkarni, N.M. Gupta, *Mater. Chem. Phys.* 17 (2009) 399–407.
- [14] M.R. Pai, J. Majeed, A.M. Banerjee, A. Arya, S. Bhattacharya, R. Rao, S.R. Bharadwaj, *J. Phys. Chem. C* 116 (2012) 1458–1471.
- [15] M.R. Pai, A.M. Singhal, A.M. Banerjee, R. Tewari, G.K. Dey, A.K. Tyagi, S.R. Bharadwaj, *J. Nanosci. Nanotechnol.* 12 (2012) 1957–1966.
- [16] TOPAS, V4.1-beta, Bruker AXS, Karlsruhe, Germany, 2004.
- [17] G. Kresse, D. Joubert, *Phys. Rev. B* 59 (1999) 1758.
- [18] P.E. Blochl, *Phys. Rev. B* 50 (1994) 17953.
- [19] J.P. Perdew, K. Burke, M. Ernzerhof, *Phys. Rev. Lett.* 77 (1996) 3865.
- [20] D. Jing, L. Guo, *J. Phys. Chem. B* 110 (2006) 11139–11145.
- [21] Z. Zhang, J.T.J. Yates, *Chem. Rev.* 112 (2012) 5520–5551.
- [22] K. Maeda, K. Teramura, T. Takata, M. Hara, N. Saito, K. Toda, Y. Inoue, H. Kobayashi, K. Domen, *J. Phys. Chem. B* 109 (2005) 20504–20510.